Material: Ferritic Steel: F82H
Property: Minimum Creep Rate vs. Applied Stress
Condition: Helium implanted
Data: Experimental

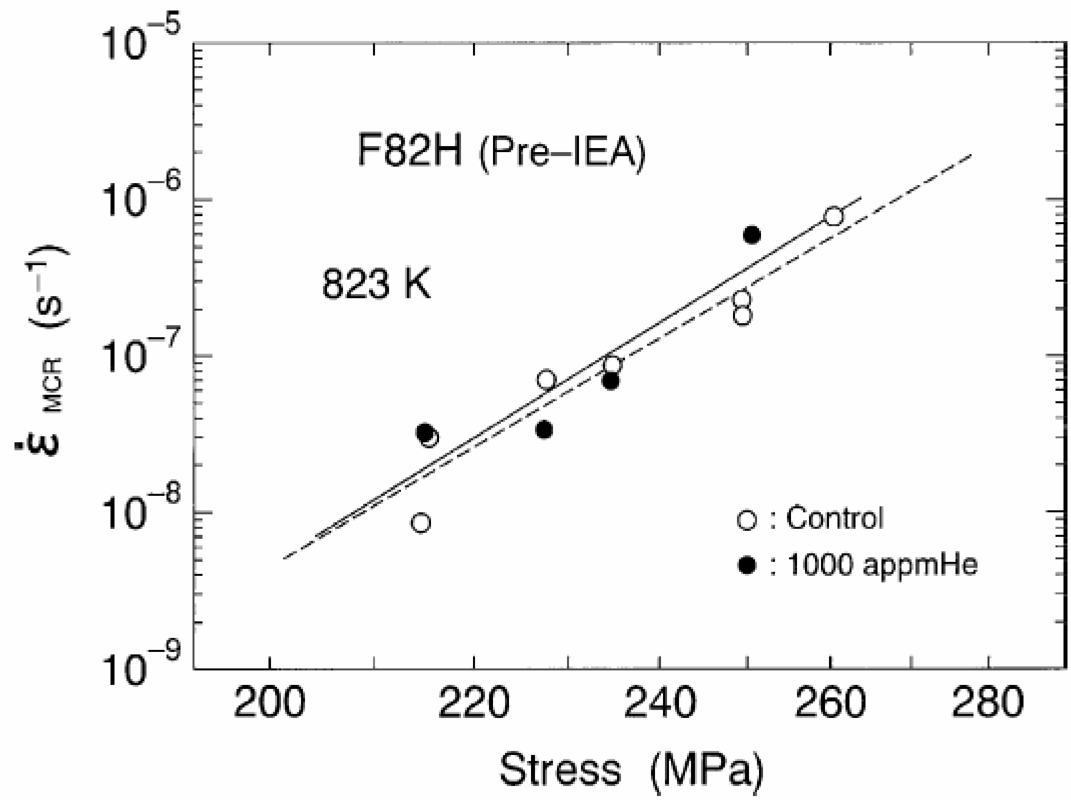

Fig. 4. Minimum creep rate as a function of applied stress for helium implanted and unimplanted F82H steel pre-IEA heat tested at 823 K.

Source:
Journal of Nuclear Materials 307-311 (2002) 217-221

Title of paper (or report) this figure appeared in:
Creep behavior of reduced activation martensitic steel F82H injected with a large amount of helium

Author of paper or graph:
N. Yamamoto, Y. Murase, J. Nagakawa, K.Shiba

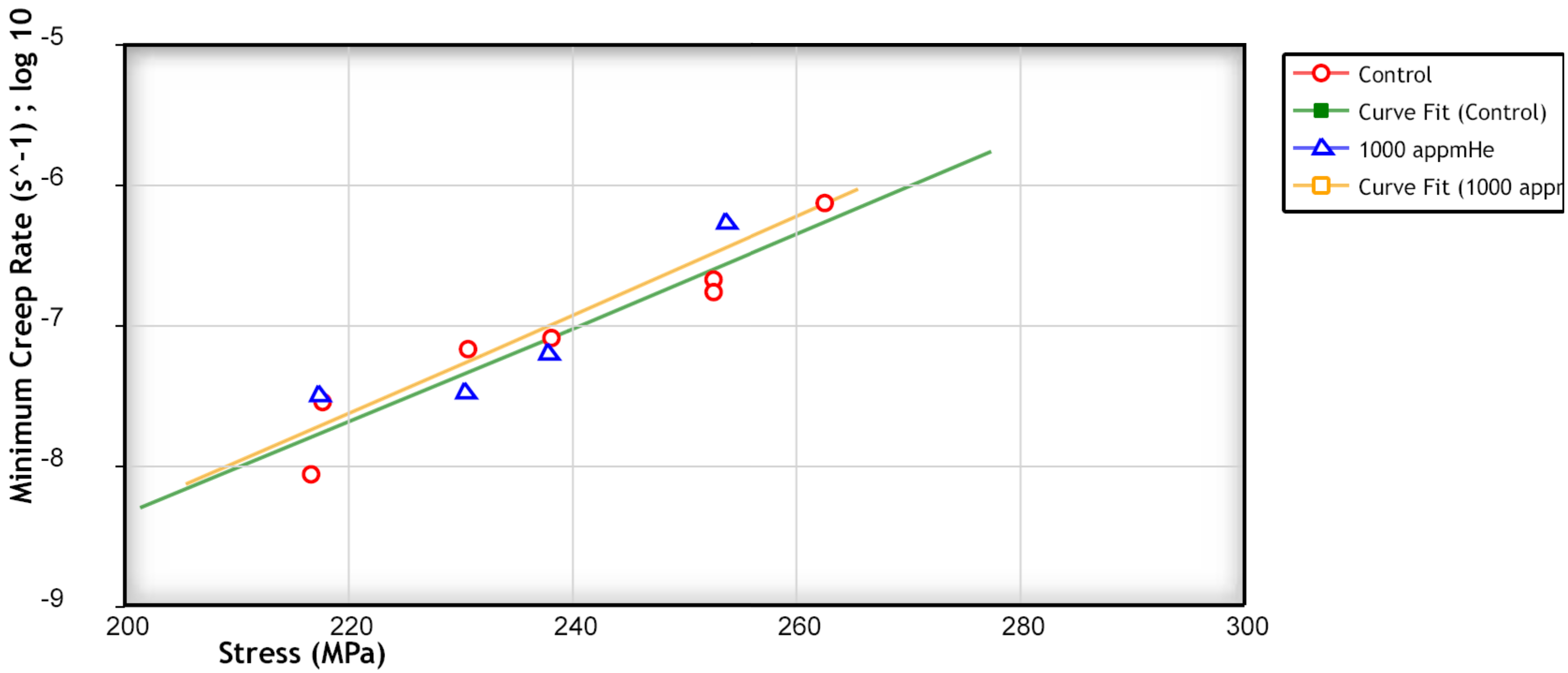

Minimum creep rate as a function of applied stress for helium implanted and unimplanted F82H steel pre-IEA heat tested at 823 K.

Reference:

Author: *N. Yamamoto, Y. Murase, J. Nagakawa, K. Shiba*

Title: *Creep behavior of reduced activation martensitic steel F82H injected with a large amount of helium*

Source: *Journal of Nuclear Materials, 2002, Volume 307-311, Page 217-221*, [PDF]

View Data

Author Comments

Plot Format:

Y-Scale: linear log ln

X-Scale: linear log ln

Journal of Nuclear Materials 307–311 (2002) 217–221

journal of nuclear materials

www.elsevier.com/locate/jnucmat

Creep behavior of reduced activation martensitic steel F82H injected with a large amount of helium

N. Yamamoto [a,*], Y. Murase [a], J. Nagakawa [a], K. Shiba [b]

[a] *National Institute for Materials Science (NIMS), 1-2-1, Sengen, Tsukuba, Ibaraki 305-0047, Japan*
[b] *Tokai Research Establishment, Japan Atomic Energy Research Institute, Tokai, Naka, Ibaraki 319-1195, Japan*

Abstract

Creep response against DEMO reactor level helium was examined on F82H steel, a candidate structural material for advanced fusion systems. Helium was injected into the material at 823 K to a concentration of about 1000 appm utilizing α-particle irradiation with a cyclotron. Post-injection creep rupture tests were conducted at the same temperature. It has been demonstrated that helium brought about no significant effect on a variety of creep properties (lifetime, rupture elongation and minimum creep rate). In parallel with this, it did not cause any influence on fracture appearance. Both helium implanted and unimplanted samples were failed in a completely transcrystalline and ductile fashion. No symptom of helium induced grain boundary separation was thereby observed even after high concentration helium introduction. These facts hint a fairly good resistance of this material toward high temperature helium embrittlement even for long-time service in fusion reactors.

1. Introduction

Neutronic generation of radioactive nuclides in materials has been commonly admitted as one of the most important problems in the field of fusion technology from the standpoint of waste management, environmental safety and public acceptance for the usage of fusion power. It is considered to get remarkably serious for advanced systems, namely DEMO reactors and beyond, on account of very high neutron doses exerted in these devices. Since this kind of activation is anticipated to take place most extensively in materials constitutive of near-plasma components, like first wall/blanket structures, the largest concern has been focussed on the development of reduced activation 'structural' materials for future reactors. Along with the low activation peculiarity, they must naturally endure to severe fusion environments, such as heavy radiation damage, and preserve mechanical integrity.

A lot of research efforts have been devoted for these 15 years so as to reply the demands mentioned above and some promising candidates are presently proposed. Amongst them the family of reduced activation martensitic steels is now regarded as the most realistic contender, chiefly owing to its maturity in industrial viewpoints [1,2]. Besides, these steels are inherited significant advantages as fusion reactor structural materials, e.g. superior thermal properties, good compatibility with coolants, and low susceptibility to void swelling and irradiation creep, from conventional Cr–Mo steels. In addition, they are considered to be tolerable against high temperature helium embrittlement, particularly as compared with austenitic steels [3]. However, unfortunately, this hypothesis has been deduced almost from short-time tests such as tensile ones and not enough corroborated through long-term examinations (creep and fatigue), whereas mechanical debasements by helium is known to be much intensified in the latter [4–6].

We have hence planned series of creep tests after hot helium implantation on a representative reduced

* Corresponding author. Tel.: +81-298 59 2554; fax: +81-298 59 2501.
E-mail address: yamamoto.norikazu@nims.go.jp (N. Yamamoto).

0022-3115/02/$ - see front matter
PII: S0022-3115(02)01182-0

activation martensitic steel, in order to clarify whether or not the above quoted favorable resistance of materials of this kind toward high temperature helium embrittlement will survive over long duration. The results on lower helium contents (100 and 300 appm He) have been already published [7]. This paper covers data on the highest concentration (1000 appm He).

2. Experimental

The material used in this experiment was a large heat (5 metric ton) of F82H steel designated as pre-IEA heat [8], the elemental composition of which is defined in Table 1. The bulk stocks of this steel were supplied by NKK Corporation in normalized (1313 K, 2.4 ks) and tempered (1013 K, 7.2 ks) condition. These treatments yielded fully martensitic structure with an austenitic grain size of 24 μm. Creep test pieces of our standard shape [9] were fabricated by spark erosion from those stocks and mechanically ground to the final thickness decided by the penetration depth of α-particles mentioned later. Their gauge section was measured 10 mm, 4 mm and 0.08 mm in length, width and thickness, respectively.

Helium injection which aimed to simulate its transmutational production in the reactor was carried out at 823 K, a maximum temperature of this material for fusion application, with an implantation rate of about 1.5×10^{-3} appm/s by means of 20 MeV α-particle bombardment from the NIMS (National Institute for Materials Science) compact cyclotron. The projected range of the α-beam was determined as 82.5 μm by SRIM 96 code [10] and could cover the sample thickness noted above. To attain a uniform helium distribution all through the specimen gauge part, the beam was scanned in two directions and its energy was moderated between 0 and 20 MeV by passing a rotating energy degrader wheel comprising aluminum foils with 16 different thicknesses which were mounted on rims of the wheel. The injected helium was amounted to 1000 appm, which roughly corresponds to accumulation at the end of blanket unit duty time in a prototype reactor [11]. To compensate temperature variation during irradiation due to beam fluctuation, an infrared lamp heater with rapid response was employed for target temperature control.

Subsequent creep rupture tests were run on at the same temperature as that of helium introduction in vacuum environment with computer installed machines of precise stress control within ±2 MPa. In order to elucidate helium effects, creep tests were also done in the same manner on unirradiated references which received anneals designed to neutralize thermal histories of helium implanted ones. The resultant rupture time reached up to around 4 Ms. After the tests, all the ruptured samples were fractographically inspected under a scanning electron microscope to mainly gain information on failure character.

Experimental details and equipment have been described in an earlier publication [9].

3. Results and discussion

Fig. 1 exemplifies creep curves of a helium bearing specimen and a non-injected companion of the material examined, which were loaded with almost the same applied stress. As seen in the figure, there would be not so much difference between the two in terms of creep deformation behavior. This feature is more generally shown in Fig. 2, in which ordinary creep-rupture plots are presented for all samples tested. The rupture strength of helium implanted pieces is in good agreement with that of unirradiated controls within the usual discrepancy of the variation of creep rupture data obtained for miniaturized thin specimens [12]. The data presented in Fig. 2 were fitted by means of usual linear regression.

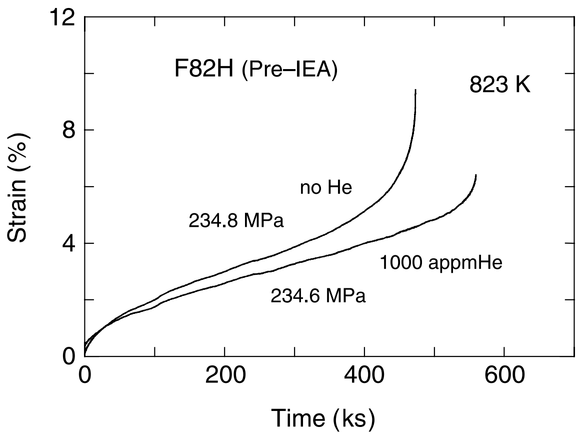

Fig. 1. Typical creep strain–time plots of helium implanted and unimplanted samples of F82H steel pre-IEA heat tested at 823 K.

Table 1
Chemical analysis of F82H steel pre-IEA heat employed in this experiment (wt%)

C	Cr	W	V	Ta	Si	Mn	P	S	Fe
0.10	7.46	2.1	0.18	0.03	0.09	0.07	0.003	0.003	Balance

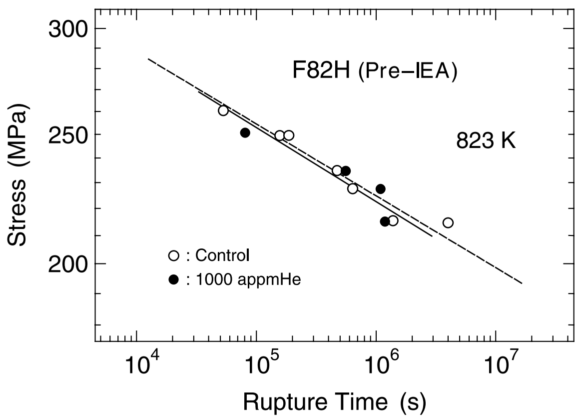

Fig. 2. Variation of rupture strength against creep lifetime for helium containing and free specimens of F82H steel pre-IEA heat tested at 823 K.

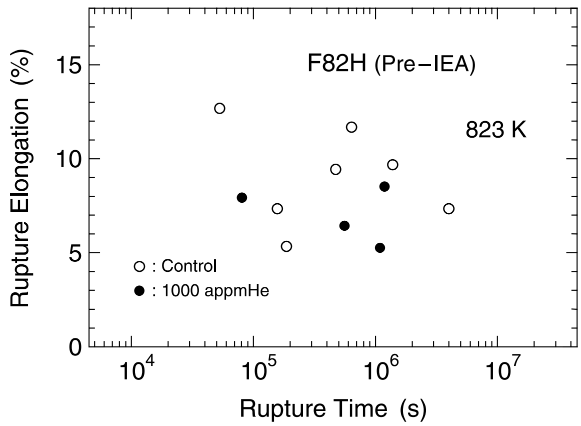

Fig. 3. Variation of rupture elongation against creep lifetime for helium containing and free specimens of F82H steel pre-IEA heat tested at 823 K.

Table 2 gives stress exponents and pre-exponential constants of the best fits based on creep power law, $t_r \propto \sigma^{-n}$, for implanted and unimplanted series. Both two coefficients revealed nearly equal values and this result once more verifies that helium introduction of 1000 appm could hardly affect the creep lifetime of F82H steel. The large values of n, alternatively strong stress dependence of rupture time, reflected a feature typical of stainless steels crept in this temperature range.

The related rupture elongation is summarizes in Fig. 3, also as a function of time to creep rupture. Though the scatter of the data points was too strong to identify any trend with respect of the rupture life, they lay within normal experimental uncertainties. The average values were $(7.0 \pm 2.9)\%$ and $(9.1 \pm 5.2)\%$ in helium injected and free conditions, respectively. There hence seems to have been no effectual deterioration of helium on elongation at rupture in common with rupture strength.

The rupture time and strain obtained here were appreciably smaller than those of ordinary sized creep test pieces (round-bar samples with 6 mm diameter) [13]. This discrepancy can be, at least partially, explained by specimen size effects [14], mainly owing to early failure in the tertiary creep stage.

The stress dependence of the minimum creep rate is compared in Fig. 4 between helium-burdened specimens and unimplanted ones. As being true for the creep lifetime and rupture elongation, helium implantation caused substantially no detrimental effect on the minimum creep rate. The results of statistical analysis on the creep power rule for this parameter, $(\mathrm{d}\varepsilon/\mathrm{d}t)_{\mathrm{MCR}} \propto \sigma^m$, listed in Table 3, also confirmed this speculation. There was no meaningful disagreement in both stress exponents and pre-exponential terms. The large values of m should mirror the strong stress dependence of rupture time previously noted.

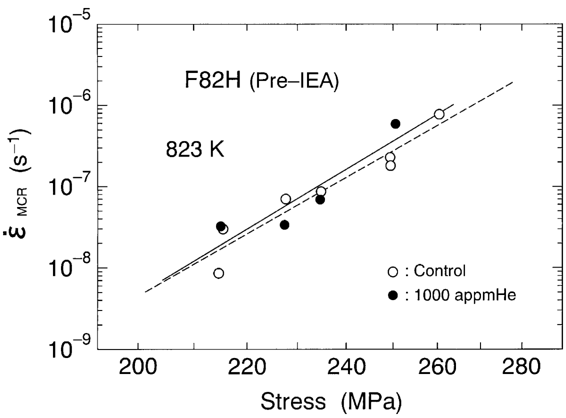

Fig. 4. Minimum creep rate as a function of applied stress for helium implanted and unimplanted F82H steel pre-IEA heat tested at 823 K.

Table 2
Stress exponent (n) and pre-exponential term (A) of creep power law fitting for creep life, $t_r \propto \sigma^{-n}$ ($\ln t_r$ (s) $= A - n \ln \sigma$ (MPa)), for helium implanted and unimplanted F82H steel pre-IEA heat at 823 K

		n	A
1000 appm He	Implanted	18.1	111
	Control	18.6	115

Table 3
Stress exponent (m) and pre-exponential term (B) of creep power law fitting for minimum creep rate, $(d\varepsilon/dt)_{MCR} \propto \sigma^m$ ($\ln(d\varepsilon/dt)_{MCR}$ (s^{-1}) $= B + m \ln \sigma$ (MPa)), for helium implanted and unimplanted F82H steel pre-IEA heat at 823 K

		m	B
1000 appm He	Implanted	19.5	−123
	Control	18.4	−117

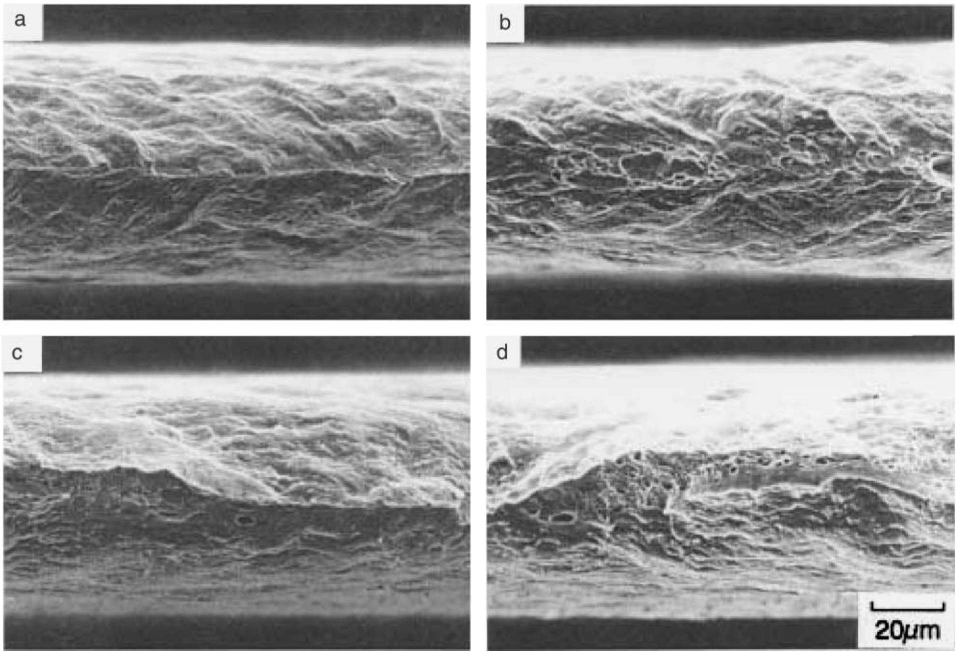

Fig. 5. SEM fractographs showing typical fracture modes of F82H steel pre-IEA heat creep-ruptured at 823 K, 235 MPa; (a) and (b) helium free reference ($t_r = 473.0$ ks); (c) and (d) helium injected sample ($C_{He} = 1000$ appm, $t_r = 559.3$ ks).

Fig. 5 shows representative ruptured faces of samples injected with 1000 appm He and their uninjected counterparts. Whereas some morphological varieties, viz. glide plane decohesion (Fig. 5(a) and (c)) and dimple fracture (Fig. 5(b) and (d)) were observed, failure modes of implanted and unimplanted materials were very similar in character, revealing the same completely intracrystalline and ductile fashion. Any kind of grain boundary embrittlement induced by helium was thereby not appreciated at all.

4. Conclusion

Influence of nuclear transmutational production of helium on long-time mechanical behavior of a typical low activation martensitic steel, F82H (pre-IEA heat [8]), was investigated by creep rupture testing at 823 K after hot implantation of fusion DEMO reactor level helium ($T_{impl.} = 823$ K, $C_{He} = 1000$ appm). The material in question demonstrated certain excellent resistance against high temperature helium embrittlement to a large helium concentration. The main facts yielding this conclusion are:

(1) No significant degradation of creep properties (creep lifetime, elongation and minimum creep rate) was arisen by helium introduction.
(2) The fracture appearance remained entirely transgranular and ductile after helium injection and there observed no indication of grain boundary separation actualized by helium.

References

[1] A. Kohyama, A. Hishinuma, Y. Kohno, K. Shiba, A. Sagara, Fus. Eng. Des. 41 (1998) 1.
[2] B. van der Schaaf, D.S. Gelles, S. Jitsukawa, A. Kimura, R.L. Klueh, A. Möslang, G.R. Odette, J. Nucl. Mater. 283–287 (2000) 52.
[3] R.L. Klueh, K. Ehrlich, F. Abe, J. Nucl. Mater. 191–194 (1992) 116.

[4] B. van der Schaaf, M.I. de Vries, J.D. Elen, in: M.L. Bleiberg, J.W. Bennett (Eds.), Proceedings of International Conference on Radiation Effects in Breeder Reactor Structural Materials, AIME, New York, 1977, p. 307.
[5] C. Wassilew, K. Ehrlich, H.-J. Bergmann, in: F.A. Garner, C.H. Henager, N. Igata (Eds.), Proceedings of 13th International Symposium (Part II) on Influence of Radiation on Material Properties, ASTM STP 956, ASTM, Philadelphia, PA, 1987, p. 30.
[6] N. Yamamoto, J. Nagakawa, H. Shiraishi, H. Kamitsubo, I. Kohno, T. Shikata, J. Nucl. Sci. Technol. 28 (1991) 1001.
[7] N. Yamamoto, J. Nagakawa, K. Shiba, J. Nucl. Mater. 283–287 (2000) 400.
[8] N. Yamanouchi, M. Tamura, H. Hayakawa, A. Hishinuma, T. Kondo, J. Nucl. Mater. 191–194 (1992) 822.
[9] N. Yamamoto, J. Nagakawa, K. Shiba, Key Eng. Mater. 171–174 (2000) 115.
[10] J.F. Ziegler, J.P. Biersack, U. Littmark, The Stopping and Range of Ions in Solids, Pergamon, New York, 1996.
[11] Y. Seki, in: Proceedings of 13th International Conference on Plasma Physics and Controlled Nuclear Fusion Research, IAEA-CN-53/G-I-2, Washington, 1990, p. 473.
[12] H. Schroeder, J. Nucl. Mater. 141–143 (1986) 476.
[13] K. Shiba, A. Hishinuma, T. Tohyama, K. Masamura, JAERI-Tech 97-038, 1997.
[14] N. Yamamoto, J. Nagakawa, K. Shiba, unpublished data.